



ARTICLE

# Optimization of Extraction, Compositional Analysis and Biological Activities of Fructus Ligustri Lucidi Essential Oil

Longgang Wang<sup>2,3,#</sup>, Xiangxun Zhuansun<sup>2,3,#</sup>, Yao Li<sup>2,3</sup>, Qili Yao<sup>2,3</sup>, Qi Liu<sup>2,3,\*</sup> and Huijing Lin<sup>1,\*</sup>

<sup>1</sup>Department of Pharmacy, The Affiliated Hospital of Yangzhou University, Yangzhou University, Yangzhou, 225009, China

<sup>2</sup>Institute of Translational Medicine, School of Medicine, Yangzhou University, Yangzhou, 225001, China

<sup>3</sup>The Key Laboratory of the Jiangsu Higher Education Institutions for Integrated Traditional Chinese and Western Medicine in Senile Diseases Control (Yangzhou University), Yangzhou, 225001, China

\*Corresponding Authors: Qi Liu. Email: liuqi@yzu.edu.cn; Huijing Lin. Email: hjlin@yzu.edu.cn

#These authors contributed equally to this work

Received: 01 December 2024; Accepted: 27 January 2025; Published: 06 March 2025

**ABSTRACT:** Fructus Ligustri Lucidi (FLL) refers to the dried mature fruit of *Ligustrum lucidum* Ait., a species from the Oleaceae family, widely distributed across East Asia and India. This study aimed to optimize the extraction process for Fructus Ligustri Lucidi essential oil (FLLO) to develop an efficient and practical extraction method. Additionally, the chemical composition of FLLO was analyzed, and its antioxidant, antimicrobial, and cytotoxic activities were evaluated. FLLO was extracted using supercritical CO<sub>2</sub> extraction, and response surface methodology was applied to optimize the extraction parameters: pressure of 16 MPa, temperature of 40°C, and extraction time of 40 min. The main components of the essential oil were identified through GC-MS analysis. Antioxidant activity was assessed using DPPH and ABTS assays, demonstrating that FLLO exhibited strong antioxidant properties, with a DPPH radical scavenging rate exceeding 80%. In antimicrobial tests, FLLO exhibited significant inhibitory effects on both Gram-positive and Gram-negative bacteria at concentrations greater than 25 mg/mL. Additionally, cytotoxicity assays revealed that FLLO enhanced the proliferation of LO2 cells. In conclusion, FLLO, extracted using supercritical CO<sub>2</sub>, demonstrates excellent antioxidant and antimicrobial properties, as well as favorable cell safety, supporting its potential for further development and application of *Ligustrum lucidum*.

**KEYWORDS:** Fructus ligustri lucidi; supercritical extraction; essential oils; safety; antibacterial activity; antioxidant activity

## 1 Introduction

Microbial contamination of food is a significant cause of human diseases [1]. Various antimicrobial agents have been incorporated into food products to inhibit microbial growth, including antibiotics, biological products, antibacterial plastics [2], fibers [3], ceramics [4,5], and metal particles [6,7]. Although antibiotics exhibit strong antibacterial activity and a broad antimicrobial spectrum, their extensive use has led to the emergence of antibiotic-resistant bacteria [8,9]. Biological products, primarily antimicrobial peptides, are costly to produce and pose concerns regarding safety and potential drug resistance [10–14]. Furthermore, the use of certain antimicrobial materials presents challenges; for instance, heavy metal ions released as antimicrobial agents can adversely affect health if improperly managed [15,16]. Consequently, natural antimicrobial substances have garnered increasing attention from researchers.



Antibacterial essential oils (EOs) are derived from natural plants and are considered preferable to antibiotics because they do not promote the development of bacterial resistance. Plant EOs have a broad range of applications and are known for their high biological safety [17], as well as the absence of residual heavy metal ions [18–21]. As a result, plant EOs have garnered significant attention from researchers in recent years. Literature reports highlight the effectiveness of EOs, such as peppermint [22], *Erigeron mucronatus* [23], and sugarcane molasses [24], which exhibit strong antibacterial activity against *Staphylococcus aureus* (*S. aureus*), *Escherichia coli* (*E. coli*), *Streptococcus pyogenes* (*S. pyogenes*), *Klebsiella pneumoniae* (*K. pneumoniae*), and other bacteria [25,26].

The extraction of plant essential oils (EOs) can be categorized into several methods: microwave-assisted extraction [27,28], steam distillation [29,30], water extraction, and alcohol extraction. While these methods are straightforward and convenient, they have certain limitations. For instance, steam distillation can only extract volatile components, while alcohol extraction may leave solvent residues. Supercritical fluid extraction (SFE) uses supercritical fluids, near their critical points, as solvents to extract the desired components from liquid or solid sources. SFE is considered a green, pollution-free, and efficient extraction method [31,32], and is particularly effective for extracting plant EOs [33,34]. Typically performed at room temperature, SFE preserves the chemical integrity of the extract. Moreover, it offers a wide extraction range with no residual solvents [35]. By adjusting different SFE conditions, high oil yields can be achieved [36,37]. EOs produced by SFE generally exhibit high biological activity [38,39].

Fructus Ligustri Lucid (FLL) is the fruit of the Oleaceae plant *Ligustrum Lucidum*, which is known for its various effects, including increasing bone mineral density [40,41], exhibiting anti-inflammatory properties [42], and protecting the liver [43,44]. However, relatively few studies have focused on the antimicrobial activities of FLL oil (FLLO). The extraction of essential oils (EOs) from FLL is typically carried out through steam distillation, water extraction, and alcohol extraction [45,46]. Supercritical CO<sub>2</sub> extraction was employed to obtain FLLO, and response surface methodology (RSM) was applied for process optimization to identify the optimal extraction conditions and analyze the product components. The antibacterial activity of FLLO was then tested. Finally, the biological safety of FLLO was evaluated by assessing its effects on liver cells (LO2). These findings provide a theoretical foundation for the development and application of FLLO in the food and pharmaceutical industries.

## 2 Materials and Methods

### 2.1 Materials

The Fructus Ligustri Lucid (FLL) used in this experiment were sourced from Tai'an, Shandong Province, China. The DPPH kit was supplied by Fuzhou Phygene Biotechnology Co., Ltd. (Fuzhou, China). The ABTS kit was obtained from Elabscience Biotechnology Co., Ltd. (Wuhan, China). And the Cell Activity Assay Kit was purchased from Beyotime Biotechnology Co., Ltd. (Shanghai, China); LO2 cells were provided by Shanghai Biowing Applied Biotechnology Co., Ltd. (Shanghai, China).

### 2.2 Supercritical Extraction Operations

The SFE apparatus (HA21-50-01) was used to extract FLLO. The procedure followed these steps: The Fructus Ligustri Lucid were crushed, sieved through a 30-mesh screen, and mixed with an equal volume of absolute ethanol; The mixture was then sealed and kept overnight. Next, 100 g of this mixture was transferred into the SFE kettle, the temperature was adjusted to the pre-set value, the carbon dioxide pump was activated, and the gas was introduced into the kettle. The pressure valve was adjusted to reach the pre-set value, and the extraction time was initiated. When the pre-set extraction time was reached, the product was collected.

## 2.3 Process Optimization

To optimize the yield of FLL, it is essential to determine the best extraction conditions for FLLO through the application of response surface methodology. Based on the results of preliminary experiments, the relationship between the independent variables—pressure ( $X_1$ ; 8–24 MPa), temperature ( $X_2$ ; 30–50°C), and time ( $X_3$ ; 30–90 min)—was evaluated, with the highest extraction efficiency of FLLO ( $Y$ ) as the dependent variable.

## 2.4 GC-MS Analysis of FLLO

For GC-MS analysis, Fructus Ligustri Lucidi essential oil was first completely dissolved in absolute ethanol, and the solution was then passed through a 0.22  $\mu\text{m}$  microporous membrane before being analyzed using an Agilent 8890–7000E triple quadrupole gas chromatograph.

The analytical conditions were as follows: a column of Agilent HP-5MS, a quartz capillary column (30 mm  $\times$  250 mm  $\times$  0.25  $\mu\text{m}$ ); helium (He) was used as the carrier gas at a flow rate of 1.2 mL/min. The injector temperature was set to 250°C, and 1  $\mu\text{L}$  of the sample was injected in split mode with a split ratio of 20:1. The temperature program started at 50°C for 2 min, then increased at a rate of 20°C/min to 220°C, held for 3 min, followed by a further increase at 30°C/min to 280°C, where it was maintained for 20 min. The total run time was 35.5 min.

For mass spectrometry, the conditions included electron impact (EI) ionization with an electron energy of 70 eV. The transmission line temperature was 250°C, and the ion source temperature was 230°C. The activation voltage was set to 15 V, and the mass scan range was from 50  $m/z$  to 500  $m/z$ . The solvent delay time was 3 min.

## 2.5 Antioxidant Activity

### 2.5.1 DPPH Method

DPPH accepts electrons from antioxidants, forming a stabilized purple free radical, which is then scavenged, resulting in a decrease in absorbance at 517 nm. Therefore, the free radical scavenging activity can be quantified by measuring the change in absorbance. A 3 mg sample of DPPH was dissolved in 100 mL of anhydrous ethanol. FLLO was then dissolved in anhydrous ethanol to obtain final concentrations of 6.25, 12.5, 25, and 50 mg/mL. Next, 100  $\mu\text{L}$  of the essential oil solution was mixed with 900  $\mu\text{L}$  of a DPPH-ethanol solution, and the reaction was allowed to proceed for 30 min at room temperature, shielded from light. The absorbance was then measured at 517 nm. For the control, 100  $\mu\text{L}$  of pure ethanol was added to 900  $\mu\text{L}$  of the DPPH-ethanol solution. The free radical scavenging activity was determined using the equation below [Eq. \(1\)](#):

$$\text{DPPH scavenging activity (\%)} = \frac{A_{\text{Control}} - A_{\text{Sample}}}{A_{\text{Control}}} \quad (1)$$

### 2.5.2 Total Antioxidant Capacity (ABTS Method)

The ABTS method is a widely used technique to assess the antioxidant capacity of a substance *in vitro*. ABTS reacts with  $\text{K}_2\text{S}_2\text{O}_8$  to form the stable free radical  $\text{ABTS}^+$ , which exhibits a maximum absorption at 734 nm and a blue-green color. When the free radicals are scavenged and reduced, the color of the solution lightens, resulting in a decrease in absorbance at 734 nm. This change can be used to determine the sample's ability to scavenge  $\text{ABTS}^+$ .

To prepare the ABTS working solution, ABTS solution and oxidant solution were mixed in a 1:1 ratio. FLLO was dissolved in anhydrous ethanol to prepare final concentrations of 6.25, 12.5, 25, and 50 mg/mL. Then, 200  $\mu$ L of the ABTS working solution and 10  $\mu$ L of FLLO were added to each well, gently mixed, and the reaction was incubated at room temperature for 2–6 min. The absorbance at 734 nm ( $A_{734}$ ) was subsequently measured and control absorbance was determined by adding distilled water to the blank wells. The total antioxidant capacity was calculated using the standard curve.

## 2.6 Antibacterial Activity

In this study, *S. aureus*, MRSA, *E. coli*, and *Salmonella* were used as test bacteria. Single colonies were inoculated into LB medium and incubated in a shaking incubator for 15 h to obtain an activated bacterial solution. Next, 50  $\mu$ L of the activated bacterial solution was added to 4950  $\mu$ L of LB liquid medium and cultured at 37°C and 180 rpm for 3 h until the optical density ( $OD_{600}$ ) reached 0.7, thereby preparing the bacterial inoculation solution. Subsequently, 900  $\mu$ L of 1% Tween-80 aqueous solution was added to 100  $\mu$ L of the bacterial inoculation solution to serve as the control group. The experimental group consisted of final FLLO concentrations of 5, 10, 25, and 50 mg/mL. After exposing the bacterial solution to different FLLO concentrations at 37°C for 24 h, 10  $\mu$ L of the solution was plated onto a Petri dish. Finally, the colony-forming units (CFU/mL) of the bacteria were counted after 12 h [47].

## 2.7 Biosafety of FLLO

### 2.7.1 Apoptosis Assay

Liver LO2 cells were initially cultured in a six-well plate ( $1 \times 10^6$  cells per well) for 24 h; FLLO was mixed with 1% Tween-80 aqueous solution, passed through a 0.22  $\mu$ m microporous membrane, and added to six-well plate to make the final concentration of the system at 50  $\mu$ g/mL, 100 mg/mL. After a 24 h incubation, the cells were treated with 1 mL of trypsin, followed by the addition of 1 mL of PBS buffer. The cells were then collected, transferred into a 5 mL centrifuge tube, and centrifuged at 800 rpm for 4 min. The supernatant was discarded, and the cell pellet was resuspended in 100  $\mu$ L of resuspension solution. Next, 5  $\mu$ L of Annexin V-FITC and 10  $\mu$ L of PI staining solution were added, and the mixture was incubated at room temperature for 15 min, protected from light. Following incubation, the cells were resuspended with an additional 400  $\mu$ L of resuspension solution. The samples were filtered through a copper mesh and analyzed using flow cytometry (BD FACSCalibur, Franklin Lake, NJ, USA), the instrument was purchased from Jiangsu New Haitian International Trading Co., Nanjing, Jiangsu Province, China. Data analysis was performed with FlowJo V10 software.

### 2.7.2 Cell Viability Assay

Cell cultures were performed in 96-well plates ( $5 \times 10^4$  cells per well). FLLO was added to the experimental group at concentrations of 12.5, 25, 50, and 100  $\mu$ g/mL, while the control group was maintained without FLLO. After 24 h of incubation, cell viability was evaluated using the CCK-8 assay. In this method, 10  $\mu$ L of CCK-8 reagent was added to each well, and the culture was continued for 2 h. Absorbance was measured at 450 nm [48], and cell viability was calculated using the following equation Eq. (2):

$$\text{Cell viability (\%)} = \frac{(\text{OD}_{\text{experiment}} - \text{OD}_{\text{blank}})}{(\text{OD}_{\text{control}} - \text{OD}_{\text{blank}})} \times 100 \quad (2)$$



## 2.8 Statistical Methods

The final results of the experiment were expressed as the mean of three replicates. The data are expressed as mean  $\pm$  standard deviation (SD) and were analyzed for statistical significance using SPSS version 26 software. Statistical significance was assessed using one-way ANOVA to compare results between different groups.

## 3 Results and Discussions

### 3.1 Optimization Results for FLLO Extraction and Its Chemical Profile

To achieve higher extraction efficiency, the Box-Behnken Design (BBD) was used for process optimization. After 17 experimental runs designed by BBD, the FLLO yield was determined, as shown in (Table 1). The corresponding surface and contour plots are also shown in (Fig. 1). Under the conditions of constant extraction time and temperature, the extraction yield of FLLO had a maximum value with the increase of pressure (Fig. 1A). When the extraction pressure and extraction time were held constant, the FLLO yield increased with higher extraction temperatures. However, once the temperature rose to 40°C, the yield increased more slowly. Under constant extraction pressure and temperature, the yield of FLLO increased as the extraction time was extended, but remained relatively unchanged when the extraction time exceeded 60 min.

**Table 1:** Experimental responses for supercritical extraction of FLLO

Experiment No.	X <sub>1</sub>	X <sub>2</sub>	X <sub>3</sub>	Response (Y)
	Pressure (MPa)	Temperature (°C)	Time (min)	Yield (%)
1	24	40	30	0.15
2	16	30	90	0.14
3	24	40	90	2.54
4	8	30	60	0.12
5	16	50	30	4.25
6	16	40	60	6.35
7	16	40	60	6.12
8	16	50	90	6.37
9	16	40	60	5.98
10	8	40	90	0.59
11	16	40	60	6.25
12	24	50	60	4.38
13	8	50	60	0.64
14	16	30	30	0.22
15	24	30	60	0.19
16	16	40	60	6.37
17	8	40	30	0.11

Final quadratic regression equation in terms of actual factors was obtained as below; also, ANOVA for quadratic model has been shown in Table 2.

$$Y = -35.64 + 1.21X_1 + 1.09X_2 + 0.18X_3 + 0.01X_1 \times X_2 + 0.01X_1 \times X_3 + 0.01X_2 \times X_3 - 0.05X_1^2 - 0.02X_2^2 - 0.01X_3^2$$

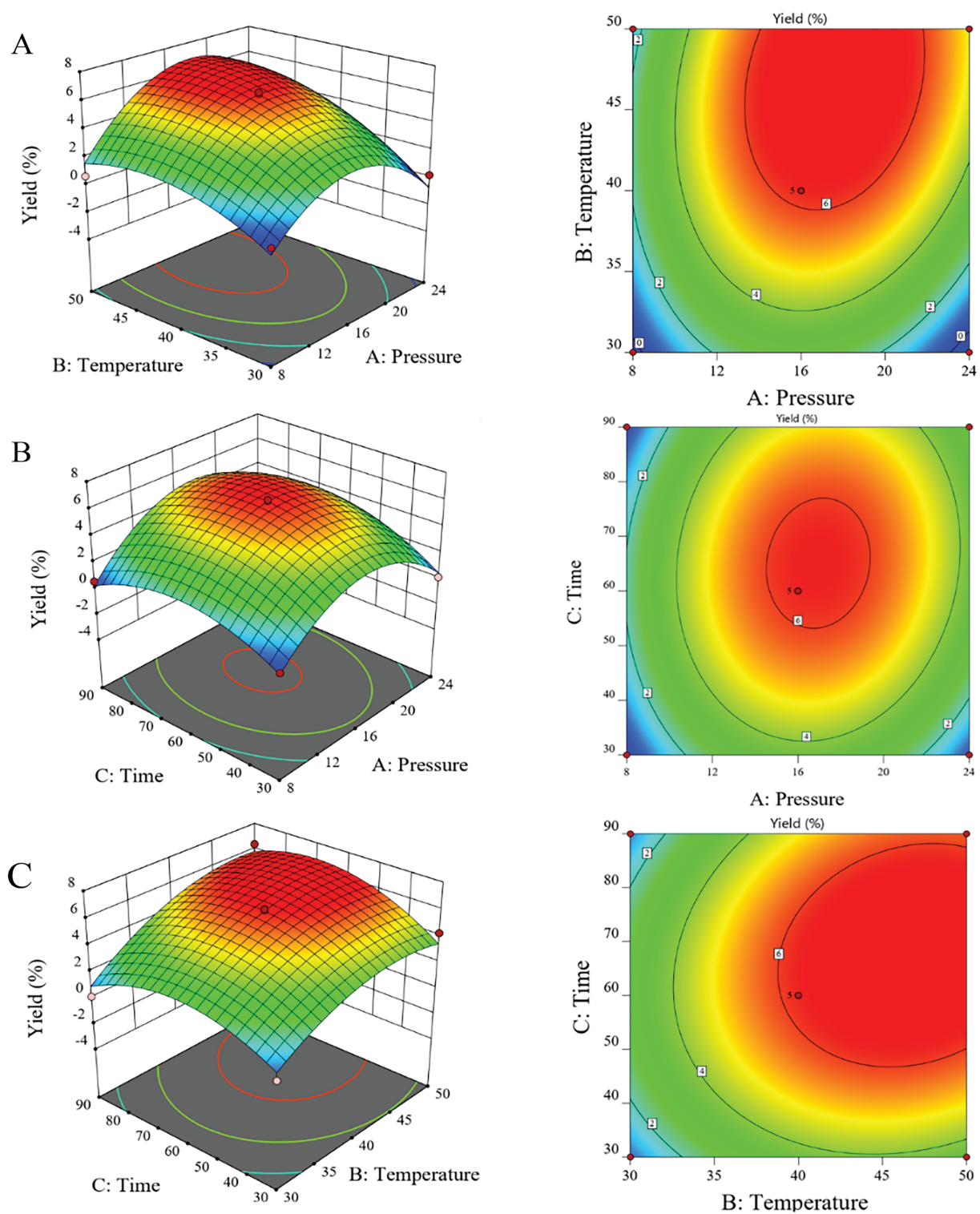


**Figure 1:** 3D response surface plots and 2D contour plots: The effects of extraction pressure and temperature (A), extraction pressure and time (B), and extraction temperature and time (C) on the yield of FLO are shown

**Table 2:** Analysis of variance (ANOVA) for the fitted quadratic model

Source	Sum of squares	DF	Mean square	F-value	p-value	Significance
Model	122.28	9	13.59	21.33	0.0003	**
X <sub>1</sub> -Pressure	4.21	1	4.21	6.60	0.0370	
X <sub>2</sub> -Temperature	28.01	1	28.01	43.98	0.0003	**
X <sub>3</sub> -Time	3.01	1	3.01	4.73	0.0661	
X <sub>1</sub> X <sub>2</sub>	3.37	1	3.37	5.29	0.0550	
X <sub>1</sub> X <sub>3</sub>	0.9120	1	0.9120	1.43	0.2704	
X <sub>2</sub> X <sub>3</sub>	1.21	1	1.21	1.90	0.2105	
X <sub>1</sub> <sup>2</sup>	48.37	1	48.37	75.95	< 0.0001	**
X <sub>2</sub> <sup>2</sup>	9.37	1	9.37	14.72	0.0064	**
X <sub>3</sub> <sup>2</sup>	16.46	1	16.46	25.84	0.0014	**
Residual	4.46	7	0.6369			
Lack of fit	4.35	3	1.45	53.85	0.0011	**
Pure error	0.1077	4	0.0269			
Cor total	126.74	16				

Note: Response 1: Yield. DF: Degree of freedom. \* indicates significant ( $p < 0.05$ ), \*\* indicates highly significant ( $p < 0.01$ ).

The optimal conditions for supercritical extraction of FLLO were determined as: The extraction was conducted at a pressure of 16 MPa, a temperature of 50°C, and an extraction time of 90 min, resulting in a yield of 6.37%. However, considering cost and safety factors, the optimal process was adjusted to: extraction pressure 16 MPa, extraction temperature 40°C, and extraction time 60 min, the extraction yield was predicted to be 6.21%. The process was then verified experimentally, and the average extraction yield of FLLO, measured across three trials, was 6.14%. Therefore, the RSM optimization for supercritical extraction of FLLO was found to be stable and feasible.

The analytical results of GC-MS are shown in (Table 3). The analysis identified 15 compounds in the essential oil of Fructus Ligustri Lucidi. Among these, terpenoids such as  $\alpha$ -Cadinol (2.67%),  $\beta$ -Sitosterol (4.65%), and Lupeol (4.88%) exhibited notable biological activities and were present in higher concentrations. Additionally, fatty acids like Palmitic Acid and Elaidic Acid, along with some alcohols, olefins, and alkanes, were detected, though in relatively lower amounts.

**Table 3:** The chemical composition of FLLO

No.	Retention time	CAS No.	Component	Relative content (% area)
1	8.398	501-94-0	4-Hydroxyphenethyl alcohol	1.23
2	9.992	481-34-5	$\alpha$ -Cadinol	2.67
3	11.807	57-10-3	Palmitic Acid	3.59
4	13.574	112-79-8	Elaidic Acid	3.94
5	14.895	7098-21-7	Tritetracontane	0.21
6	15.348	301-02-0	Oleamide	0.66
7	16.084	112-95-8	Icosane	0.49

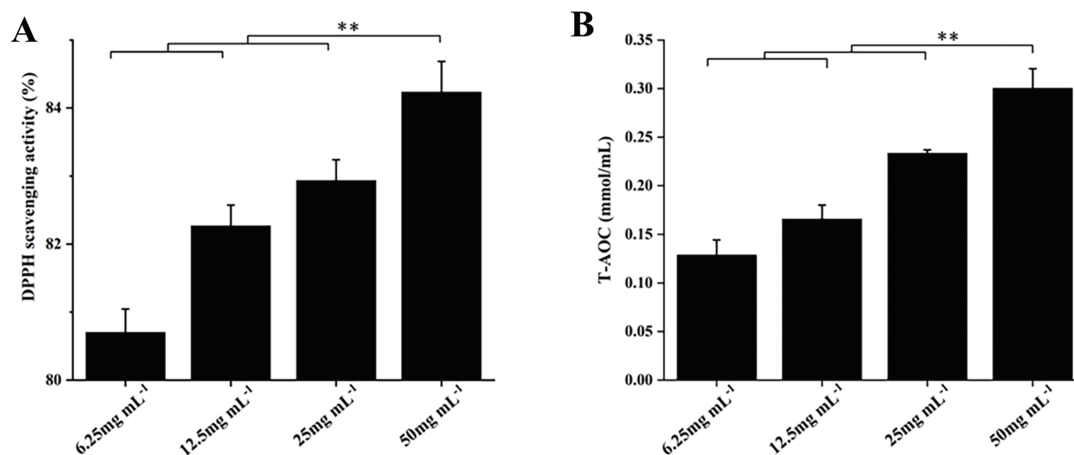
(Continued)

Table 3 (continued)

No.	Retention time	CAS No.	Component	Relative content (% area)
8	16.934	53057-53-7	1,21-Docosadiene	3.04
9	17.352	297-03-0	Cyclotetracosane	2.14
10	18.473	506-42-3	Elaidyl Alcohol	3.71
11	22.171	59-02-9	Vitamin E	0.12
12	25.695	83-46-5	$\beta$ -Sitosterol	4.65
13	27.591	545-47-1	Lupeol	4.88
14	30.382	1617-68-1	Lupeol acetate	1.06
15	32.588	5989-08-2	$\alpha$ -Longipinene	5.12

### 3.2 Antioxidant Activity

Plant essential oils, as natural products, generally exhibit strong antioxidant activity. Their antioxidant capacity is affected by factors such as the type, composition, and concentration of the essential oil, making them widely applicable in fields such as medicine and food. Fig. 2 below illustrates the antioxidant activity of FLLO measured using two methods. Both methods showed the same trend, the antioxidant capacity increased with higher concentrations of essential oil concentration, and the DPPH radical scavenging activity exceeded 80%. This suggests that FLLO has excellent antioxidant activity, likely attributed to the high concentrations of  $\beta$ -Sitosterol and Lupeol, as indicated by the GC-MS data in Table 3. These findings are consistent with the work of Parvez et al. [49].



**Figure 2:** DPPH scavenging activity of FLLO (A); Total antioxidant capacity of FLLO (B). \*\* indicates highly significant ( $p < 0.01$ )

### 3.3 Antibacterial Activity

In the next step, the antibacterial activity of the optimum FLLO was evaluated against four different bacteria: *S. aureus*, MRSA, *E. coli*, and *Salmonella*. The results revealed that FLLO exhibited significant antibacterial activity against these target bacteria (Fig. 3), with no major differences in activity among the four bacteria. At final FLLO concentrations of 5 and 10 mg/mL, bacterial numbers were slightly reduced compared to the control group. However, at a concentration of 25 mg/mL, a significant reduction in bacterial

numbers was observed ( $p < 0.05$ ). Finally, at a concentration of 50 mg/mL, no bacterial growth was detected (Fig. 3). These findings suggest that FLLO has a strong antibacterial effect against the tested bacteria, likely due to the high concentration of  $\alpha$ -Cadinol in FLLO. A study by Su et al. also reported strong antibacterial activity of  $\alpha$ -Cadinol derived from the fruit essential oil of *Eucalyptus citriodora* [50].

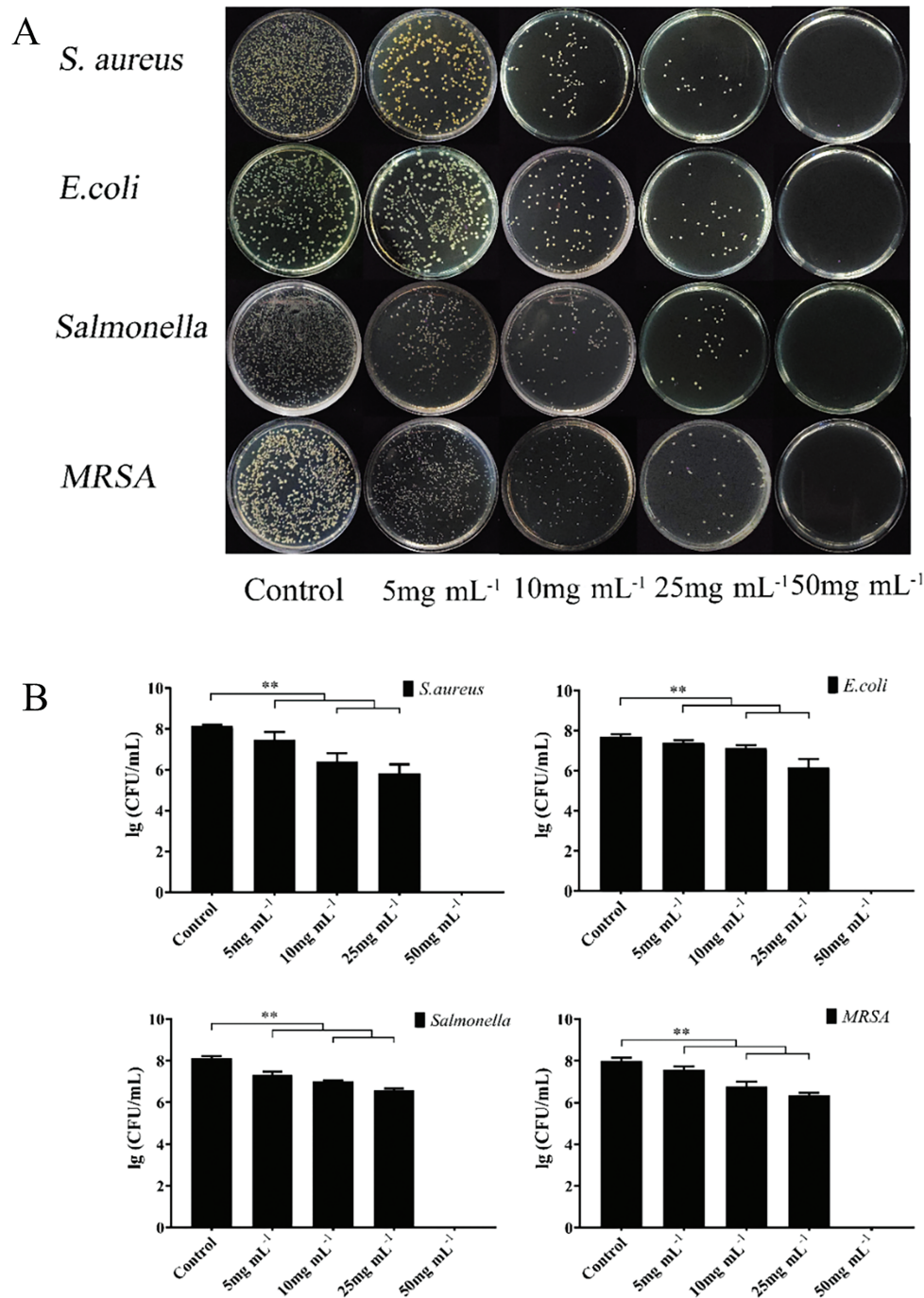


**Figure 3:** Bacterial growth after treatment with various concentrations of FLLO (A); The inhibitory effect of FLLO against different bacteria (B). \*\* indicates highly significant ( $p < 0.01$ )



### 3.4 In Vitro Cytotoxicity of FLLO

Based on the results of the study, it was found that FLLO exhibits good antimicrobial and antioxidant activities, indicating its great potential for future applications in both pharmaceutical and food fields. To ensure the biosafety of FLLO, hepatocytes (LO2) were chosen to investigate the effects of different concentrations of FLLO on cell viability and apoptosis.

#### 3.4.1 Apoptosis Results

Annexin V-FITC/PI staining was employed to evaluate the effect of FLLO on apoptosis in LO2 cells [51]. The results demonstrated that FLLO effectively inhibited both early and late apoptosis in LO2 cells. At a concentration of 50  $\mu\text{g/mL}$ , the early and late apoptosis rates were 4.12% and 1.75%, respectively. When the FLLO concentration was increased to 100  $\mu\text{g/mL}$ , the early and late apoptosis rates were 3.89% and 1.63%, respectively. In contrast, the early and late apoptosis rates in the control group were 6.41% and 2.51%, respectively. These findings suggest that FLLO effectively protects hepatocyte growth and demonstrates good biosafety while maintaining its potent antibacterial activity.

#### 3.4.2 Viability Results

As a potential antimicrobial additive, the safety of FLLO is crucial. Cytotoxicity serves as an important indicator for evaluating the biological safety of antimicrobial compounds. As shown in (Fig. 4), after 24 h of FLLO treatment, the cell survival rate at a concentration of 12.5  $\mu\text{g/mL}$  was  $\geq 80\%$ , and at concentrations of 25  $\mu\text{g/mL}$  or higher, the cell survival rate increased to  $\geq 100\%$ . The results demonstrate exhibits good safety in LO2 cells. This may be related to the presence of ursolic acid in FLLO, which was shown by Zhou et al. to have the potential to promote the proliferation and differentiation of LO2 cells [4,52].

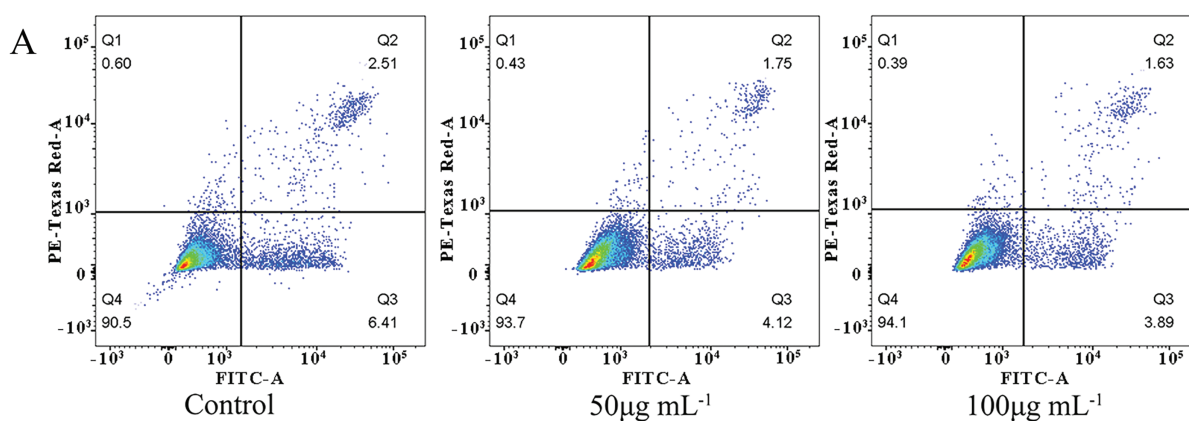
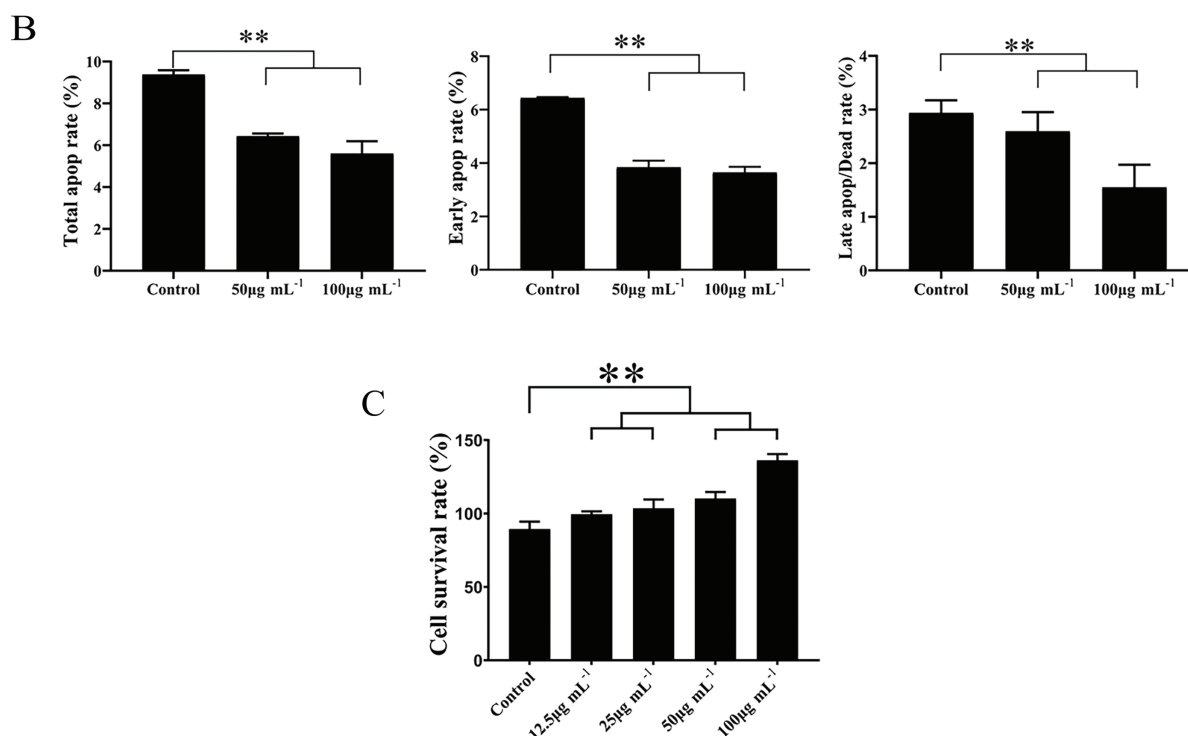


Figure 4: (Continued)





**Figure 4:** The effect of FLLO on LO2 cell apoptosis in different concentrations (A); and different phase (B); Cell viability of LO2 cells after treatment with FLLO for 24 h (C). \*\* indicates highly significant ( $p < 0.01$ )

## 4 Conclusions

These findings demonstrate that FLLO is a naturally derived compound with excellent antioxidant and antibacterial properties, coupled with a high safety profile in LO2 cells. As such, FLLO holds significant potential as an additive in food, pharmaceutical, and cosmetic applications. Moreover, the extraction process was optimized using supercritical carbon dioxide extraction to enhance efficiency. However, to fully realize the benefits and broader applicability of FLLO, further research is needed. This should include *in vivo* studies and evaluations against a broader range of bacterial and fungal strains, facilitating the development of more effective and safer antimicrobial agents. Additionally, future studies should focus on comprehensive chemical analyses of FLLO to identify its active components with antioxidant and antimicrobial properties and elucidate their mechanisms of action.

**Acknowledgement:** Thank you for the professional testing services provided by the Yangzhou University Test Center.

**Funding Statement:** The authors received no specific funding for this study.

**Author Contributions:** Longgang Wang: Methodology; Formal analysis; Data curation; Writing—original draft preparation. Xiangxun Zhuansun: Methodology; Formal analysis; Data curation; Writing—original draft preparation. Yao Li: Methodology; Software; Qili Yao: Methodology; Qi Liu: Conceptualization; Investigation; Writing—review and editing; Supervision; Project administration. Huijing Lin: Project administration; Supervision. All authors reviewed the results and approved the final version of the manuscript.

**Availability of Data and Materials:** Not applicable.

**Ethics Approval:** Not applicable.

**Conflicts of Interest:** The authors declare no conflicts of interest to disclose concerning the present study.

## References

1. Abebe GM. The role of bacterial biofilm in antibiotic resistance and food contamination. *Int J Microbiol.* 2020;2020:1–10. doi:10.1155/2020/1705814.
2. Chang SH, Chen YJ, Tseng HJ, Hsiao HI, Chai HJ, Shang KC, et al. Antibacterial activity of chitosan-poly lactate fabricated plastic film and its application on the preservation of fish fillet. *Polymers.* 2021;13(5):696. doi:10.3390/polym13050696.
3. Pagnotta G, Graziani G, Baldini N, Maso A, Focarete ML, Berni M, et al. Nanodecoration of electrospun polymeric fibers with nanostructured silver coatings by ionized jet deposition for antibacterial tissues. *Mat Sci Eng C.* 2020;113. doi:10.1016/j.msec.2020.110998.
4. Verma AS, Singh A, Kumar D, Dubey AK. Electro-mechanical and polarization-induced antibacterial response of 45S5 bioglass-sodium potassium niobate piezoelectric ceramic composites. *Acs Biomater Sci Eng.* 2020;6(5):3055–69. doi:10.1021/acsbomaterials.0c00091.
5. Zhu TL, Zhu M, Zhu YF. Fabrication of forsterite scaffolds with photothermal-induced antibacterial activity by 3D printing and polymer-derived ceramics strategy. *Ceram Int.* 2020;46(9):13607–14. doi:10.1016/j.ceramint.2020.02.146.
6. Bieganski P, Szczupak L, Arruebo M, Kowalski K. Brief survey on organometalated antibacterial drugs and metal-based materials with antibacterial activity. *RSC Chem Biol.* 2021;2(2):368–86. doi:10.1039/D0CB00218F.
7. Qi Y, Ren SS, Che Y, Ye JW, Ning GL. Research progress of metal-organic frameworks based antibacterial materials. *Acta Chim Sinica.* 2020;78(7):613–24. doi:10.6023/A20040126.
8. Mitcheltree MJ, Myers AG. Bacterial drug resistance overcome by synthetic restructuring of antibiotics. *Nature.* 2021. doi:10.1038/d41586-021-02916-6.
9. Kasew D, Eshetie S, Diress A, Tegegne Z, Moges F. Multiple drug resistance bacterial isolates and associated factors among urinary stone patients at the University of Gondar Comprehensive Specialized Hospital, Northwest Ethiopia. *BMC Urol.* 2021;21(1):27. doi:10.1186/s12894-021-00794-8.
10. Liu JY, Li HX, Li HZ, Fang SF, Shi JG, Chen YZ, et al. Rational design of dipicolylamine-containing carbazole amphiphiles combined with Zn<sup>2+</sup> as potent broad-spectrum antibacterial agents with a membrane-disruptive mechanism. *J Med Chem.* 2021;64(14):10429–444. doi:10.1021/acs.jmedchem.1c00858.
11. Alhaji NB, Isola TO. Antimicrobial usage by pastoralists in food animals in North-central Nigeria: The associated socio-cultural drivers for antimicrobials misuse and public health implications. *One Health.* 2018;6:41–7. doi:10.1016/j.onehlt.2018.11.001.
12. Gao X, Li HX, Niu XH, Zhang DY, Wang Y, Fan HY, et al. Carbon quantum dots modified Ag<sub>2</sub>S/CS nanocomposite as effective antibacterial agents. *J Inorg Biochem.* 2021;220. doi:10.1016/j.jinorgbio.2021.111456.
13. Wu VM, Tang S, Uskokovic V. Calcium phosphate nanoparticles as intrinsic inorganic antimicrobials: The antibacterial effect. *Acs Appl Mater Inter.* 2018;10(40):34013–28. doi:10.1021/acsami.8b12784.
14. Fan YF, Chen HF, Mu N, Wang WG, Zhu KK, Ruan Z, et al. Nosiheptide analogues as potential antibacterial agents via dehydroalanine region modifications: Semi-synthesis, antimicrobial activity and molecular docking study. *Bioorgan Med Chem.* 2021;31. doi:10.1016/j.bmc.2020.115970.
15. Wronska N, Katir N, Milowska K, Hammi N, Nowak M, Kedzierska M, et al. Antimicrobial effect of chitosan films on food spoilage bacteria. *Int J Mol Sci.* 2021;22(11):5839. doi:10.3390/ijms22115839.
16. Díez-Pascual AM. Antimicrobial polymer-based materials for food packaging applications. *Polymers.* 2020;12(4):731. doi:10.3390/polym12040731.
17. de Medeiros VM, do Nascimento YM, Souto AL, Madeiro SAL, Costa VCD, Silva SMPM, et al. Chemical composition and modulation of bacterial drug resistance of the essential oil from leaves of *Croton grewioides*. *Microb Pathog.* 2017;111:468–71. doi:10.1016/j.micpath.2017.09.034.

18. Luo M, Tang L, Dong Y, Huang H, Deng Z, Sun Y. Antibacterial natural products lobophorin L and M from the marine-derived *Streptomyces* sp. 4506. *Nat Prod Res.* 2021;35(24):5581–7. doi:10.1080/14786419.2020.1797730.
19. Rajesh P, Saravanan G, Muthusami MS, Hariprasath L. “Natural products chemistry and drug design-2020”—a thematic issue (part-3). *Cardiovasc Hematol Agents Med Chem.* 2021;19(2):100. doi:10.2174/187152571902210805111421.
20. An P, Zhang LJ, Peng W, Chen YY, Liu QP, Luan X, et al. Natural products are an important source for proteasome regulating agents. *Phytomedicine.* 2021;93:153799. doi:10.1016/j.phymed.2021.153799.
21. Arshad N, Hameed A, Hashim J, Iqbal T, Munir I, Ali SA, et al. Natural products embedded crown ethers as potent insulin secretory agents. *Pak J Pharm Sci.* 2021;34(5):2003–8.
22. Ciotea D, Shamtsyan M, Popa ME. Antibacterial activity of peppermint, basil and rosemary essential oils obtained by steam distillation. *Agrolife Sci J.* 2021;10(1):75–82. doi:10.17930/AGL.
23. Awen BZ, Unnithan CR, Ravi S, Lakshmanan AJ. GC-MS analysis, antibacterial activity and genotoxic property of essential oil. *Nat Prod Commun.* 2010;5(4):621–4. doi:10.1177/1934578X1000500426.
24. Zhang K, Ding ZD, Mo MM, Duan WJ, Bi YG, Kong FS. Essential oils from sugarcane molasses: chemical composition, optimization of microwave-assisted hydrodistillation by response surface methodology and evaluation of its antioxidant and antibacterial activities. *Ind Crops Prod.* 2020;156:112875. doi:10.1016/j.indcrop.2020.112875.
25. Ahmadi S, Fazilati M, Nazem H, Mousavi SM. Green synthesis of magnetic nanoparticles using *satureja hortensis* essential oil toward superior antibacterial/fungal and anticancer performance. *BioMed Res Int.* 2021;2021. doi:10.1155/2021/8822645.
26. Insawang S, Pripdeevech P, Tanapichatsakul C, Khruengsai S, Monggoot S, Nakham T, et al. Essential oil compositions and antibacterial and antioxidant activities of five *Lavandula stoechas* cultivars grown in Thailand. *Chem Biodivers.* 2019;16(10). doi:10.1002/cbdv.201900371.
27. Spinozzi E, Pavela R, Bonacucina G, Perinelli DR, Cespi M, Petrelli R, et al. Spilanthal-rich essential oil obtained by microwave-assisted extraction from *Acmella oleracea* (L.) RK Jansen and its nanoemulsion: insecticidal, cytotoxic and anti-inflammatory activities. *Ind Crops Prod.* 2021;172:114027. doi:10.1016/j.indcrop.2021.114027.
28. Sharma M, Hussain S, Shalima T, Aav R, Bhat R. Valorization of seabuckthorn pomace to obtain bioactive carotenoids: An innovative approach of using green extraction techniques (ultrasonic and microwave-assisted extractions) synergized with green solvents (edible oils). *Ind Crops Prod.* 2022;175:114257. doi:10.1016/j.indcrop.2021.114257.
29. El Kharraf S, El-Guendouz S, Farah A, Bennani B, Mateus MC, El Hadrami E, et al. Hydrodistillation and simultaneous hydrodistillation-steam distillation of *Rosmarinus officinalis* and *Origanum compactum*: antioxidant, anti-inflammatory, and antibacterial effect of the essential oils. *Ind Crops Prod.* 2021;168:113591. doi:10.1016/j.indcrop.2021.113591.
30. Xiao Y, Liu ZZ, Gu HY, Yang FJ, Zhang L, Yang L. Improved method to obtain essential oil, asarinin and sesamin from *Asarum heterotropoides* var. *mandshuricum* using microwave-assisted steam distillation followed by solvent extraction and antifungal activity of essential oil against *Fusarium* spp. *Ind Crops Prod.* 2021;162:113295. doi:10.1016/j.indcrop.2021.113295.
31. Men Y, Fu SP, Xu C, Zhu YM, Sun YX. Supercritical fluid CO<sub>2</sub> extraction and microcapsule preparation of *Lycium barbarum* residue oil rich in zeaxanthin dipalmitate. *Foods.* 2021;10(7):1468. doi:10.3390/foods10071468.
32. Shen J, Shen W, Cai X, Wang JX, Zheng MX. High performance liquid chromatographic method for determination of active components in lithospermum oil and its application to process optimization of lithospermum oil prepared by supercritical fluid extraction. *Chin J Chromatogr.* 2021;39(7):708–14. doi:10.3724/sp.j.1123.2020.12009.
33. Mihalcea L, Turturica M, Cuculea EI, Danila GM, Dumitrascu L, Coman G, et al. CO supercritical fluid extraction of oleoresins from sea buckthorn pomace: evidence of advanced bioactive profile and selected functionality. *Antioxidants.* 2021;10(11):1681. doi:10.3390/antiox10111681.
34. Atiqah MSN, Gopakumar DA, Owolabi FAT, Pottathara YB, Rizal S, Aprilia NAS, et al. Extraction of cellulose nanofibers via eco-friendly supercritical carbon dioxide treatment followed by mild acid hydrolysis and the fabrication of cellulose nanopapers. *Polymers.* 2019;11(11):1813. doi:10.3390/polym11111813.

35. Cerón-Martínez LJ, Hurtado-Benavides AM, Ayala-Aponte A, Serna-Cock L, Tirado DF. A pilot-scale supercritical carbon dioxide extraction to valorize colombian mango seed kernel. *Molecules*. 2021;26(8):2279. doi:10.3390/molecules26082279.
36. Vidovic S, Tomsik A, Vladic J, Jokic S, Aladic K, Pastor K, et al. Supercritical carbon dioxide extraction of *Allium ursinum*: Impact of temperature and pressure on the extracts chemical profile. *Chem Biodivers*. 2021;18(4):e2100058. doi:10.1002/cbdv.202100058.
37. Hassim N, Markom M, Rosli MI, Harun S. Scale-up approach for supercritical fluid extraction with ethanol-water modified carbon dioxide on *Phyllanthus niruri* for safe enriched herbal extracts. *Sci Rep*. 2021;11(1):15818. doi:10.1038/s41598-021-95222-0.
38. Dimic I, Pezo L, Rakic D, Teslic N, Zekovic Z, Pavlic B. Supercritical fluid extraction kinetics of cherry seed oil: kinetics modeling and ANN optimization. *Foods*. 2021;10(7):1513. doi:10.3390/foods10071513.
39. Lee JH, Lee YY, Lee J, Jang YJ, Jang HW. Chemical composition, antioxidant, and anti-inflammatory activity of essential oil from omija (*Schisandra chinensis* (Turcz.) Baill.) produced by supercritical fluid extraction using CO<sub>2</sub>. *Foods*. 2021;10(7):1619. doi:10.3390/foods10071619.
40. Wu Y, Hu YS, Zhao ZG, Xu LN, Chen Y, Liu TT, et al. Protective effects of water extract of *Fructus Ligustri Lucidi* against oxidative stress-related osteoporosis *in vivo* and *in vitro*. *Vet Sci*. 2021;8(9):198. doi:10.3390/vetsci8090198.
41. Liu HX, Guo YB, Zhu RY, Wang LL, Chen BB, Tian YM, et al. Fructus Ligustri Lucidi preserves bone quality through induction of canonical Wnt/ $\beta$ -catenin signaling pathway in ovariectomized rats. *Phytother Res*. 2021;35(1):424–41. doi:10.1002/ptr.6817.
42. Kim YJ, Park SY, Koh YJ, Lee JH. Anti-neuroinflammatory effects and mechanism of action of Fructus ligustri lucidi extract in BV2 microglia. *Plants*. 2021;10(4):688. doi:10.3390/plants10040688.
43. Lu Q, Xing HZ, Yang NY. Mass spectrometry-based label-free quantitative proteomic analysis of CCl<sub>4</sub>-induced acute liver injury in mice intervened by total glycosides from Ligustri Lucidi Fructus. *Curr Proteomics*. 2021;18(3):338–48. doi:10.2174/1570164617999200728192812.
44. Yang NY, Zhang YW, Guo JM. Preventive effect of total glycosides from against nonalcoholic fatty liver in mice. *Z Naturforsch C*. 2015;70(9–10):237–41. doi:10.1515/znc-2015-4161.
45. Li G, Zhang XA, Zhang JF, Chan CY, Yew DTW, He ML, et al. Ethanol extract of promotes osteogenesis of mesenchymal stem cells. *Phytother Res*. 2010;24(4):571–6. doi:10.1002/ptr.2987.
46. Sha NN, Zhao YJ, Zhao DF, Mok DKW, Shi Q, Wang YJ, et al. Effect of the water fraction isolated from Fructus Ligustri Lucidi extract on bone metabolism antagonizing a calcium-sensing receptor in experimental type 1 diabetic rats. *Food Funct*. 2017;8(12):4703–12. doi:10.1039/C7FO01259D.
47. Shen XY, Ma RN, Huang YX, Chen L, Xu ZB, Li DD, et al. Nano-decocted ferrous polysulfide coordinates ferroptosis-like death in bacteria for anti-infection therapy. *Nano Today*. 2020;35:100981. doi:10.1016/j.nantod.2020.100981.
48. Bunchongprasert K, Shao J. Effect of fatty acid ester structure on cytotoxicity of self-emulsified nanoemulsion and transport of nanoemulsion droplets. *Colloid Surface B*. 2020;194:111220. doi:10.1016/j.colsurfb.2020.111220.
49. Parvez MK, Alam P, Arbab AH, Al-Dosari MS, Alhowiriny TA, Alqasoumi SI. Analysis of antioxidative and antiviral biomarkers  $\beta$ -amyrin,  $\beta$ -sitosterol, lupeol, ursolic acid in *Guiera senegalensis* leaves extract by validated HPTLC methods. *Saudi Pharm J*. 2018;26(5):685–93. doi:10.1016/j.jsps.2018.02.022.
50. Su YC, Hsu KP, Composition Ho CL. Composition, in vitro antibacterial and anti-mildew fungal activities of essential oils from twig and fruit parts of eucalyptus citriodora. *Nat Prod Commun*. 2017;12(10):1647–50. doi:10.1177/1934578X1701201031.
51. Zhao HY, Chen SX, Hu KZ, Zhang ZF, Yan XR, Gao HJ, et al. 5-HTP decreases goat mammary epithelial cells apoptosis through MAPK/ERK/Bcl-3 pathway. *Gene*. 2021;769:145240. doi:10.1016/j.gene.2020.145240.
52. Zhou ML, Yi YP, Liu L, Lin Y, Li J, Ruan JH, et al. Polymeric micelles loading with ursolic acid enhancing anti-tumor effect on hepatocellular carcinoma. *J Cancer*. 2019;10(23):5820–31. doi:10.7150/jca.30865.